EMBO
reports

TG2 regulates the heat-shock response by the post-translational modification of HSF1

Federica Rossin[1], Valeria Rachela Villella[2], Manuela D'Eletto[1], Maria Grazia Farrace[1], Speranza Esposito[2], Eleonora Ferrari[2], Romina Monzani[2], Luca Occhigrossi[1], Vittoria Pagliarini[3,4], Claudio Sette[3,4], Giorgio Cozza[5], Nikolai A Barlev[6], Laura Falasca[7], Gian Maria Fimia[7,8], Guido Kroemer[9,10,11,12,13,14,15] (iD), Valeria Raia[16], Luigi Maiuri[2,17] & Mauro Piacentini[1,7,*] (iD)

Abstract

Heat-shock factor 1 (HSF1) is the master transcription factor that regulates the response to proteotoxic stress by controlling the transcription of many stress-responsive genes including the heat-shock proteins. Here, we show a novel molecular mechanism controlling the activation of HSF1. We demonstrate that transglutaminase type 2 (TG2), dependent on its protein disulphide isomerase activity, triggers the trimerization and activation of HSF1 regulating adaptation to stress and proteostasis impairment. In particular, we find that TG2 loss of function correlates with a defect in the nuclear translocation of HSF1 and in its DNA-binding ability to the HSP70 promoter. We show that the inhibition of TG2 restores the unbalance in HSF1-HSP70 pathway in cystic fibrosis (CF), a human disorder characterized by deregulation of proteostasis. The absence of TG2 leads to an increase of about 40% in CFTR function in a new experimental CF mouse model lacking TG2. Altogether, these results indicate that TG2 plays a key role in the regulation of cellular proteostasis under stressful cellular conditions through the modulation of the heat-shock response.

Introduction

Transglutaminase type 2 (TG2) is a multifunctional, ubiquitously expressed member of the TG family that catalyses post-translational modifications of proteins through both Ca^{2+}-dependent and Ca^{2+}-independent reactions [1]. Several unique features, including its ubiquitous expression, widespread localization, binding to and hydrolysis of guanine nucleotides, distinguish TG2 from the other transglutaminases [2]. Indeed, in addition to its crosslinking activity, TG2 might also act as a GTP-binding protein that mediates intracellular signalling by coupling the alpha-1 beta-adrenergic receptor to phospholipase C-gamma 1 [3,4]. Substantial evidence indicates that under physiological circumstances the enzyme may also act as protein disulphide isomerase (PDI). In the last few years, it has been established that TG2 switches its 3D structure from a nucleotide-bound "closed" to the transamidation/PDI prone "open" conformation [5,6]. These 3D changes influence the interaction of TG2 with multiple substrates or binding partners that are essential to carry out its biological functions [7]. The peculiar biochemistry of this enzyme as well as its capacity to interact with the main proteins involved in the regulation of proteostasis suggests that TG2 plays a key role in this process. For example, among the TG2 intracellular partners, many are molecular chaperones, such as the heat-shock proteins HSP70, HSP27, HSP90 as well as co-chaperone from the DNAjs and the BAG families [7–10]. Indeed, recent compelling evidence places TG2 within the regulation of main pathways

1 Department of Biology, University of Rome 'Tor Vergata', Rome, Italy
2 Division of Genetics and Cell Biology, European Institute for Research in Cystic Fibrosis, San Raffaele Scientific Institute, Milan, Italy
3 Department of Biomedicine and Prevention, University of Rome 'Tor Vergata', Rome, Italy
4 Laboratory of Neuroembryology, Fondazione Santa Lucia, Rome, Italy
5 Department of Molecular Medicine, University of Padua, Padova, Italy
6 Gene Expression Laboratory, Institute of Cytology, Saint-Petersburg, Russia
7 National Institute for Infectious Diseases IRCCS 'L. Spallanzani', Rome, Italy
8 Department of Biological and Environmental Sciences and Technologies (DiSTeBA), University of Salento, Lecce, Italy
9 Sorbonne Paris Cité, Université Paris Descartes, Paris, France
10 Equipe 11 labellisée Ligue Nationale contre le Cancer, Centre de Recherche des Cordeliers, Paris, France
11 Institut National de la Santé et de la Recherche Médicale, U1138, Paris, France
12 Université Pierre et Marie Curie, Paris, France
13 Metabolomics and Cell Biology Platforms, Gustave Roussy Cancer Campus, Villejuif, France
14 Pôle de Biologie, Hôpital Européen Georges Pompidou, AP-HP, Paris, France
15 Department of Women's and Children's Health, Karolinska University Hospital, Stockholm, Sweden
16 Regional Cystic Fibrosis Center, Pediatric Unit, Department of Translational Medical Sciences, Federico II University, Naples, Italy
17 SCDU of Pediatrics, Department of Health Sciences, University of Piemonte Orientale, Novara, Italy
*Corresponding author. Tel: +39 0672 594234; E-mail: mauro.piacentini@uniroma2.it

controlling the proteome homeostasis as autophagy, proteasome and exosomes [11–14]. In keeping with this, there is a vast literature describing the deregulation of this enzyme during the pathogenesis of major human diseases (neurodegenerative, liver and respiratory disorders as well as cancer) [15–17] in which there is a deregulated proteostasis that can be improved by modulators of TG2 activity [18,19]. In spite of differences related to cell- and tissue-specific disease context, these disorders share common features of unbalanced cell adaptation to either cell autonomous or environmental stress. Thus, TG2 can be viewed as a dynamic platform that aims at restoring cellular imbalances. However, it remains elusive through which mechanisms the TG2-mediated capability of fighting stress is disrupted, making TG2 a harmful, instead of beneficial, player in disease pathogenesis. Several TG2 inhibitors can ameliorate disease phenotype, either in pre-clinical or in clinical settings [20]. One typical example is cysteamine, a small molecule with pleiotropic functions, among which the capability of inhibiting TG2 transamidating activity, with proved to have beneficial pre-clinical or clinical effects in neurodegenerative disorders [15,21], fibrosis [16] as well as in cystic fibrosis (CF) [17]. Cysteamine is capable of controlling the consequences of TG2 overactivation in CF, improving the trafficking of the most common misfolded F508del CFTR mutant [17,22–25].

Here, we demonstrate that TG2 regulates proteostasis and the general cellular adaptation to stress. By combining *in vivo* approaches in transgenic mice with *in vitro* studies, we demonstrate that TG2, by acting as a PDI, is able to activate HSF1, the master transcriptional regulator of the stress-responsive genes. We show that TG2 controls the heat-shock response by modulating the expression of the stress-inducible chaperone HSP70. Moreover, we report that cysteamine inhibits the PDI activity of TG2, restoring the proteostasis imbalance in CF, a finding that might explain its superior activity as a therapeutic agent.

Results

HSP70 expression is dependent on TG2 both *in vivo* and *in vitro*

We have previously demonstrated that TG2 is involved in the assembly and clearance of ubiquitinated aggregates [12]. In addition, the enzyme interacts with several molecular chaperones and proteins involved in the folding machinery [7] including the stress-inducible form of HSP70 (HSPA1A). Based on these findings, we evaluated the hypothesis of whether TG2 might influence proteostasis by modulating the chaperone homeostasis. To this aim, we analysed the effect of TG2 ablation on HSP70 induction. First, mice that were either wild type or knockout for TG2 (TG2$^{+/+}$ and TG2$^{-/-}$ mice) were exposed to hyperthermic stress at 42°C for 20 min to stimulate heat-shock response and HSP70 induction. HSP70 protein expression was examined in different tissues (Fig 1) after heat shock (HS) or 1 and 3 h after recovery at room temperature. Immunoblotting revealed that mice lacking TG2 had a significant defect in HSP70 induction in all the examined organs (Fig 1A–D). We next confirmed this result *in vitro*, using mouse embryonic fibroblasts (MEFs) from TG2$^{+/+}$ and TG2$^{-/-}$ mice. To validate the *in vivo* data, TG2$^{+/+}$ and TG2$^{-/-}$ MEFs, as well as TG2$^{-/-}$ MEFs stably reconstituted with the unmutated TG2 (TG2$^{-/-}$ MEF^{TG2}), were either exposed to heat shock for 20, 40, 60 min (Fig 2A) or treated

with the proteasome inhibitor MG132 (Fig 2B). Both treatments are known to cause the accumulation of misfolded proteins and the consequent induction of HSP70 [26–28]. As shown in Fig 2A and B, in the absence of TG2, no induction of HSP70 occurred after HS or proteasome inhibition. Interestingly, the reintroduction of human TG2 into TG2$^{-/-}$ MEF was sufficient to rescue HSP70 induction. Similarly, shRNA-mediated silencing of TG2 in TG2$^{+/+}$ MEF significantly reduced the induction of HSP70 by heat shock (Fig 2C). Commensurate with a key role for TG2 and HSP70 in the recovery from stress, TG2$^{+/+}$ MEF exhibited a transient increase in protein ubiquitination post-HS, suggesting successful clearance of damaged proteins, while TG2$^{-/-}$ MEF showed a stable elevation of protein ubiquitination (Fig 2D). Moreover, in contrast to TG2$^{+/+}$ MEF, the lack of HSP70 induction in TG2$^{-/-}$ MEF correlated to HS-dependent apoptosis as highlighted by the activation of caspase 3 (Fig EV1).

TG2 mediates HSF1 activation

In order to define the molecular mechanism regulating the TG2-dependent induction of HSP70, we focused our attention on the heat-shock factor 1 (HSF1), the main transcription factor involved in HSP70 expression. Activation of HSF1, associated with hyperphosphorylation, requires a multi-step process that includes the translocation into the nucleus, the transition from a monomeric to a trimeric form and the binding to target gene promoters [29–31]. To verify whether the lack of HSP70 induction, in absence of TG2, was due to a defect in the HSF1 activation, we first analysed the nuclear translocation of the transcriptional factor after HS (Fig 3A and B) and proteasome inhibition with MG132 (Fig 3C and D), two cellular stresses known to activate the transcriptional response mediated by HSF1. As expected [32–34], in TG2$^{+/+}$ MEF HSF1 was only present in the cytosol in basal conditions and rapidly translocated into the nucleus after heat shock or MG132 addition leading to HSP70 expression (Fig 3A–D). By contrast, the lack of HSP70 induction in TG2$^{-/-}$ MEF was correlated to a significant decrease in the nuclear translocation of HSF1 (Fig 3B and D). Interestingly, the amount of hyperphosphorylated HSF1, shortly after heat shock, was reduced in TG2$^{-/-}$ MEF as compared to TG2$^{+/+}$ MEF (Fig 3E). Moreover, while HSF1 hyperphosphorylation was transient in TG2$^{+/+}$ MEF, it persisted also during the recovery phase in TG2$^{-/-}$ MEF. These results indicate that TG2 is required for the optimal activation of HSF1.

To characterize how TG2 could modulate HSF1 activation, we first verified whether the two proteins could interact. Co-immunoprecipitation analyses revealed that TG2 interacts with HSF1 just after HS (Fig 4A and B). This result was also confirmed by immunofluorescence microscopy showing the co-localization of TG2 and HSF1 in the nucleus after HS (Fig 4C and D).

To bind DNA and transactivate target genes, HSF1 must trimerize following the formation of disulphide bonds between cysteine residues [35,36]. The formation of three intermolecular S-S bonds between two cysteine residues (Cys36 and Cys103) is essential for HSF1 trimerization and DNA binding. However, so far the mechanism by which Cys36 and Cys103 form this intermolecular S-S bond was elusive. Considering that TG2 interacts with HSF1 after HS, we asked whether the enzyme, through its PDI activity, would trigger HSF1 trimerization leading to its activation. To this aim, we analysed the trimerization of HSF1 in TG2$^{+/+}$ and TG2$^{-/-}$ MEF after heat shock (Fig 5A) or proteasome inhibition (Fig 5B) using or not
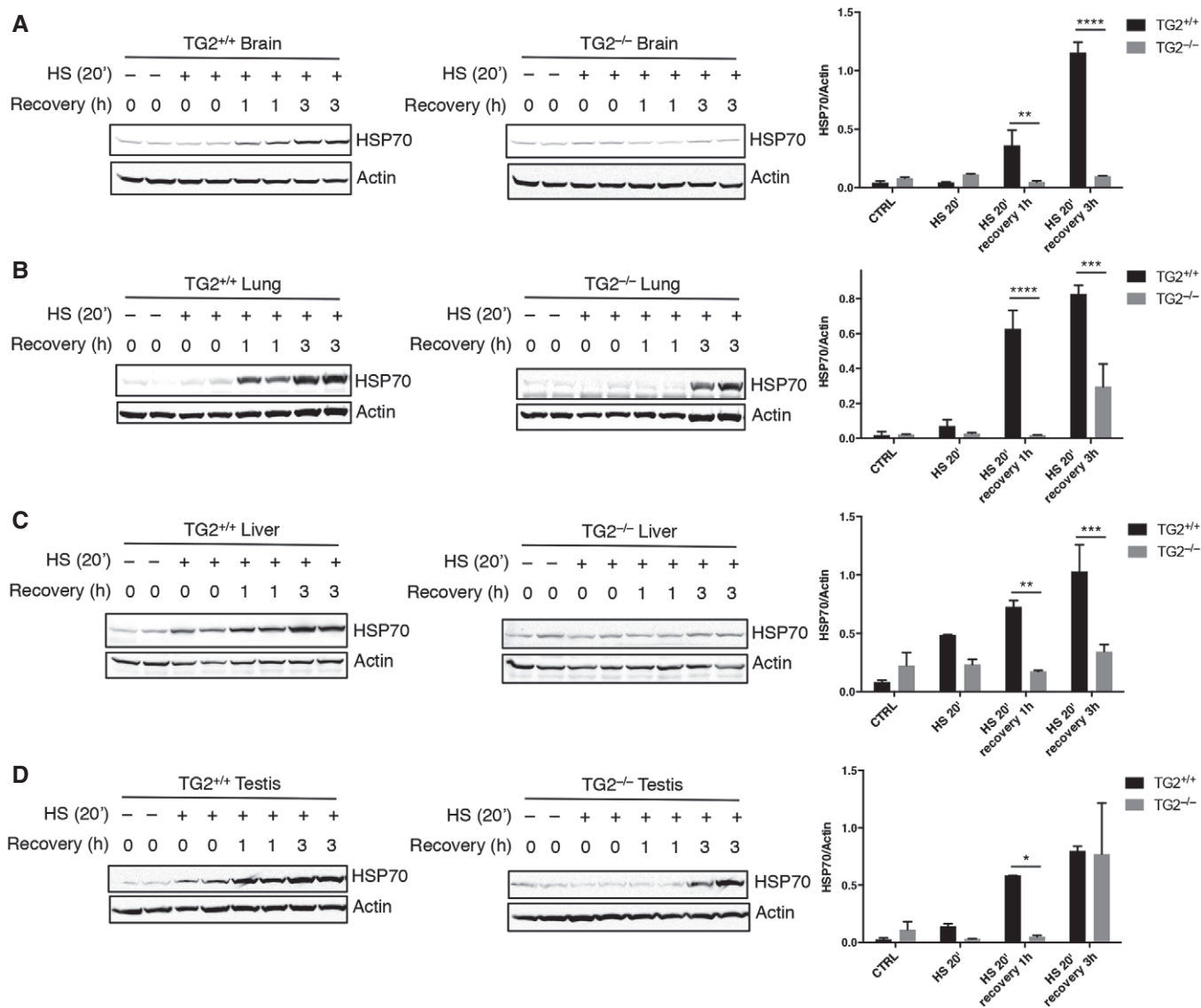
Figure 1. The ablation of TG2 leads to a defect in the induction of HSP70 protein expression in mice tissues after exposure to a proteotoxic stress (HS).

A–D   Western blot and densitometric analysis of HSP70 protein levels in brain (A), lung (B), liver (C) and testis (D) tissues from TG2$^{+/+}$ and TG2$^{-/-}$ mice after exposure to heat shock at 42°C for 20 min. HSP70 expression was also monitored after 1 and 3 h of recovery at 37°C. Actin was used as loading control.

Data information: Results are mean ± SEM of three independent experiments; *$P < 0.05$; **$P < 0.01$; ***$P < 0.001$; ****$P < 0.0001$ (one-way ANOVA).

reducing agents. Interestingly, heat shock and proteasome inhibition induced the trimerization of HSF1 (molecular weight 240 kDa) only in TG2$^{+/+}$ MEF, without reducing condition (Fig 5A and B), and this reaction was confined to the nuclear pool of HSF1 (Fig EV2A and B). Next, we performed an *in vitro* assay using recombinant TG2 and HSF1 proteins (Fig 5C) to show that TG2 effectively induced HSF1 polymerization. HSF1 polymerized only if it was phosphorylated and in the absence of calcium, which is known to interfere with the redox-sensitive cysteines of TG2 and consequently with its PDI activity [37]. Importantly, the regulation of HSF1-HSP70 pathway by TG2 occurs through its PDI activity and not the transamidating one. In fact, the treatment with Z-DON, a specific inhibitor of the transamidating activity of TG2, affects neither

HSP70 induction nor HSF1 nuclear translocation after proteasome inhibition (Fig EV2C). These data suggest that TG2 PDI activity induces the trimerization of HSF1, which in turn facilitates transactivation of the HSP70 gene by binding to heat-shock elements (HSEs) in the promoter. To confirm this hypothesis, we analysed the DNA-binding ability of HSF1 to the HSP70 promoter in the presence and absence of TG2 by chromatin immunoprecipitation (ChIP) assay. We found that HSF1 was recruited to the HSP70 promoter after heat shock in TG2$^{+/+}$ but not in TG2$^{-/-}$ MEF (Fig 5D). Accordingly, quantification of HSP70 mRNA indicated that the HSP70 gene was efficiently transcribed only in TG2$^{+/+}$ MEF in response to HS (Fig 5E). Altogether, these results reveal that TG2 promotes HSF1 trimerization in heat-stressed cells, thereby
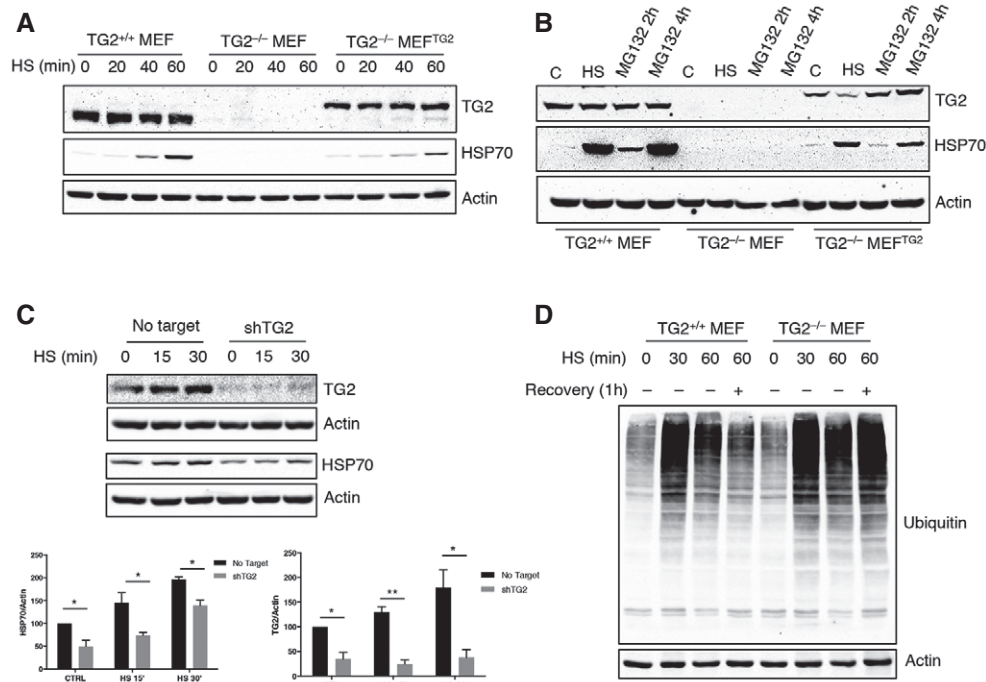
Figure 2. HSP70 induction is dependent on TG2 both after heat shock and after proteasome inhibition.

A, B   Western blot analysis of HSP70 and TG2 protein levels in TG2$^{+/+}$ MEF, TG2$^{-/-}$ MEF and TG2$^{-/-}$ MEF^{TG2} after heat shock for 20, 40 and 60 min (A) or proteasome inhibition with MG132 for 2 and 4 h (B). Actin was used as loading control.
C   Western blot and densitometric analysis of HSP70 and TG2 in TG2$^{+/+}$ MEF silenced for TG2 (shTG2) after exposure to heat shock. Actin was used as loading control.
D   Western blot analysis of ubiquitinated proteins after exposure of TG2$^{+/+}$ and TG2$^{-/-}$ MEF to a heat shock for 30 and 60 min or 60 min followed by 1 h of recovery to 37°C. Actin was used as loading control.

Data information: Results are mean ± SEM of three independent experiments; *$P < 0.05$; **$P < 0.01$ (one-way ANOVA).

stimulating HSF1-mediated transactivation of the HSP70 gene. TG2 dependent activation of HSF1 also regulates the expression of other target genes such as BAG3 and HSP25 (Fig EV2D). Thus, these findings demonstrate a key role played by TG2 in the control of cellular stress homeostasis via the post-translational modification of HSF1.

TG2 ablation in CF mice restores F508del CFTR function

One sign of perturbed proteostasis that accompanies CF is the overexpression of HSP70 protein that associates with mutated CFTR [38,39]. Moreover, active trimeric HSF1 and several of its target chaperones are increased in CF cells and favour the degradation of mutated CFTR protein [40,41]. In contrast to wild-type CFTR, F508del CFTR is unable to dissociate from HSP70 and consequently rapidly degraded by the proteasome [38,39].

To translate our findings *in vivo* and elucidate the molecular mechanisms by which TG2 regulates CF pathogenesis, we developed a new experimental mouse model carrying the F508 CFTR deletion on a TG2 null background. We used the mouse model to test the effects of TG2 ablation on the capacity of F508del CFTR mice of counteracting luminal challenges, either in the intestine or in the airways. Mice homozygous for F508del mutations often died within the first week of life and the majority of the survivors succumbed to the intestinal obstruction just after weaning (between 21 and 28 days), if they were kept on standard chow [24]. We first characterized the

new mouse model in terms of survival immediately after birth, and we found that CF mice on TG2 null background (CFTR^{F508del}/TG2$^{-/-}$) mice not only were born at the expected Mendelian frequency (Fig EV3) but, fed with a standard diet, survived after weaning (Fig 6A). Subsequently, we analysed the sensitivity of these mice to the infection with *Pseudomonas aeruginosa*, a persistent bacteria that commonly infects and kills CF patients as a result of chronic lung inflammation. To this aim, mice were infected by intratracheal instillation of the *P. aeruginosa* PAO1 strain and either sacrificed 1 day later, to surgically collect the lungs and measure bacterial clearance, or kept in an isolator to monitor their survival. WT (CFTR^{wt}/TG2$^{+/+}$) and CF mice on TG2 null background (CFTR^{F508del}/TG2$^{-/-}$) indistinguishable survived in response to PAO1 infection, while CFTR homozygous ones (CFTR^{F508del}/TG2$^{+/+}$) succumbed to infection (Fig 6B). Moreover, CFTR^{F508del}/TG2$^{-/-}$ mice cleared *P. aerguinosa* more efficiently from their lungs than CFTR^{F508del}/TG2$^{+/+}$ animals (Fig 6C). As a surrogate of inflammation, we measured the RNA levels of TNF-α in different tissue. TNF-α mRNA was reduced in the lungs and intestines from CFTR^{F508del}/TG2$^{-/-}$ mice as compared to mice with the CFTR^{F508del}/TG2$^{+/+}$ genotype, indicating that the increased inflammation, usually observed in CF mice, was reduced when TG2 was absent (Fig 6D). These results suggest that TG2 ablation improves the overall conditions of CF mice. Finally, we measured CFTR-dependent chloride secretion *ex vivo* in segment of the ileum mounted in Ussing chambers. This CFTR activity was defined as a forskolin-induced increase
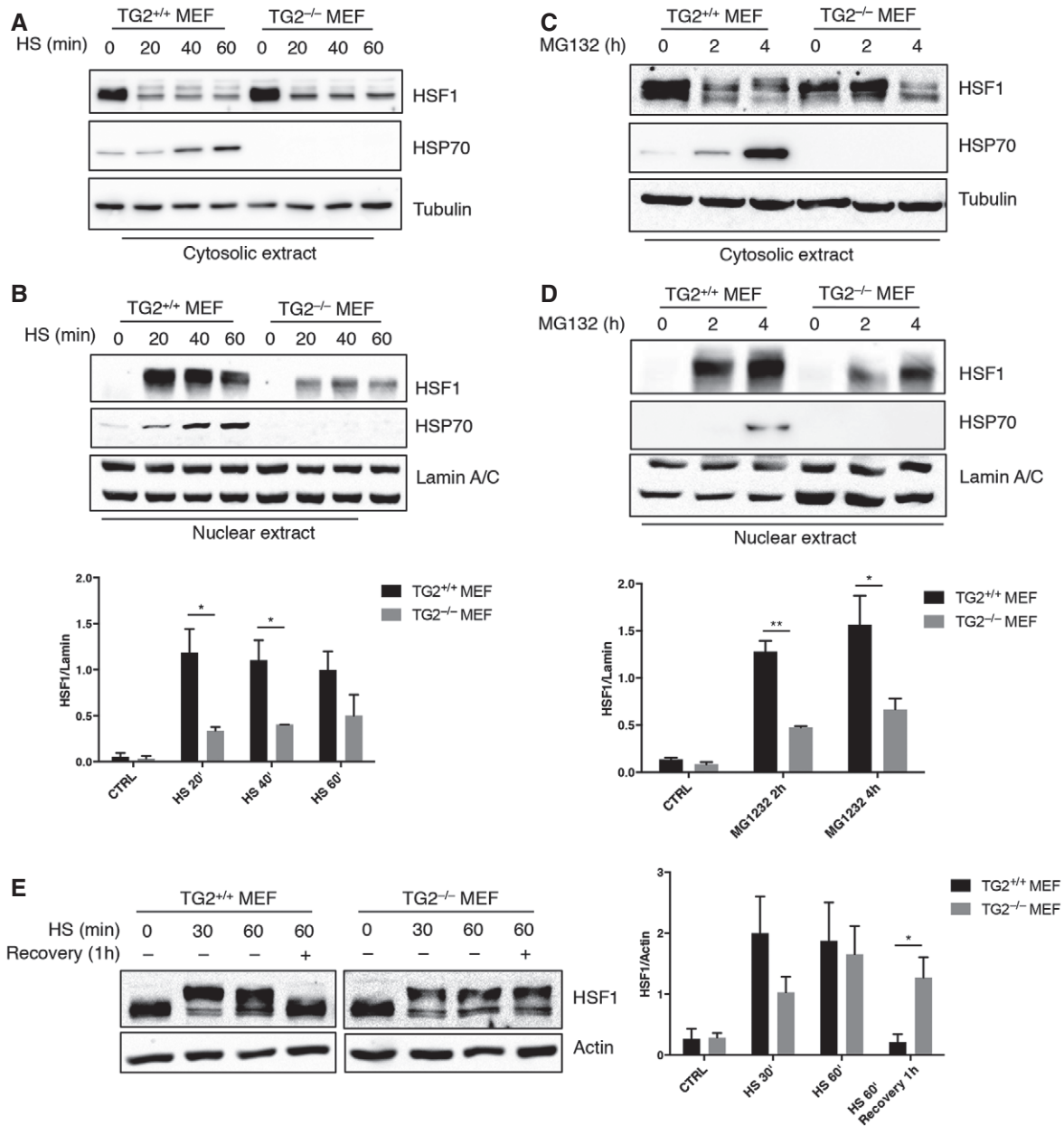
Figure 3. TG2 protein levels affect HSF1 nuclear translocation and phosphorylation.

A–D   Western blot analysis of HSF1 nuclear translocation and subsequent HSP70 expression in cytosolic and nuclear fractions of TG2$^{+/+}$ and TG2$^{-/-}$ MEF treated with heat shock for 20, 40 and 60 min (A, B) and MG132 for 2 and 4 h (C, D). Tubulin was used as loading control for cytosolic extract. Lamin A/C was used as loading control for nuclear extract. Densitometric analysis of nuclear HSF1 amount after HS and MG132 in TG2$^{+/+}$ and TG2$^{-/-}$ MEF.

E   Western blot analysis of HSF1 expression in whole-cell lysates of TG2$^{+/+}$ and TG2$^{-/-}$ MEF after 30 and 60 min of heat shock or 60 min followed by 1 h of recovery to 37°C. The hyperphosphorylation-dependent shift of HSF1 can be detected after HS. Actin was used as loading control. Densitometric analysis of the HSF1 hyperphosphorylated form after HS in TG2$^{+/+}$ and TG2$^{-/-}$ MEF.

Data information: Results are mean ± SEM of three independent experiments; *$P < 0.05$; **$P < 0.01$ (one-way ANOVA).

in short-circuit current (Isc) that was partially reverted by a selective CFTR inhibitor (CFTRinh172, Fig 6E), in line with previous publications [17]. While CFTR^{F508del}/TG2$^{+/+}$ mice were devoid of CFTR function, CFTR^{F508del}/TG2$^{-/-}$ mice exhibited approximately 40% of the CFTR activity found in wild-type controls, thus indicating that the CFTR function was partially restored (Fig 6E).

TG2 is involved in CF pathogenesis by regulating HSP70-HSF1 pathway

The above-reported findings prompted us to investigate whether the effects of TG2 on HSF1-mediated HSP70 transactivation may contribute to CF pathogenesis in the mouse model. Intestinal HSP70
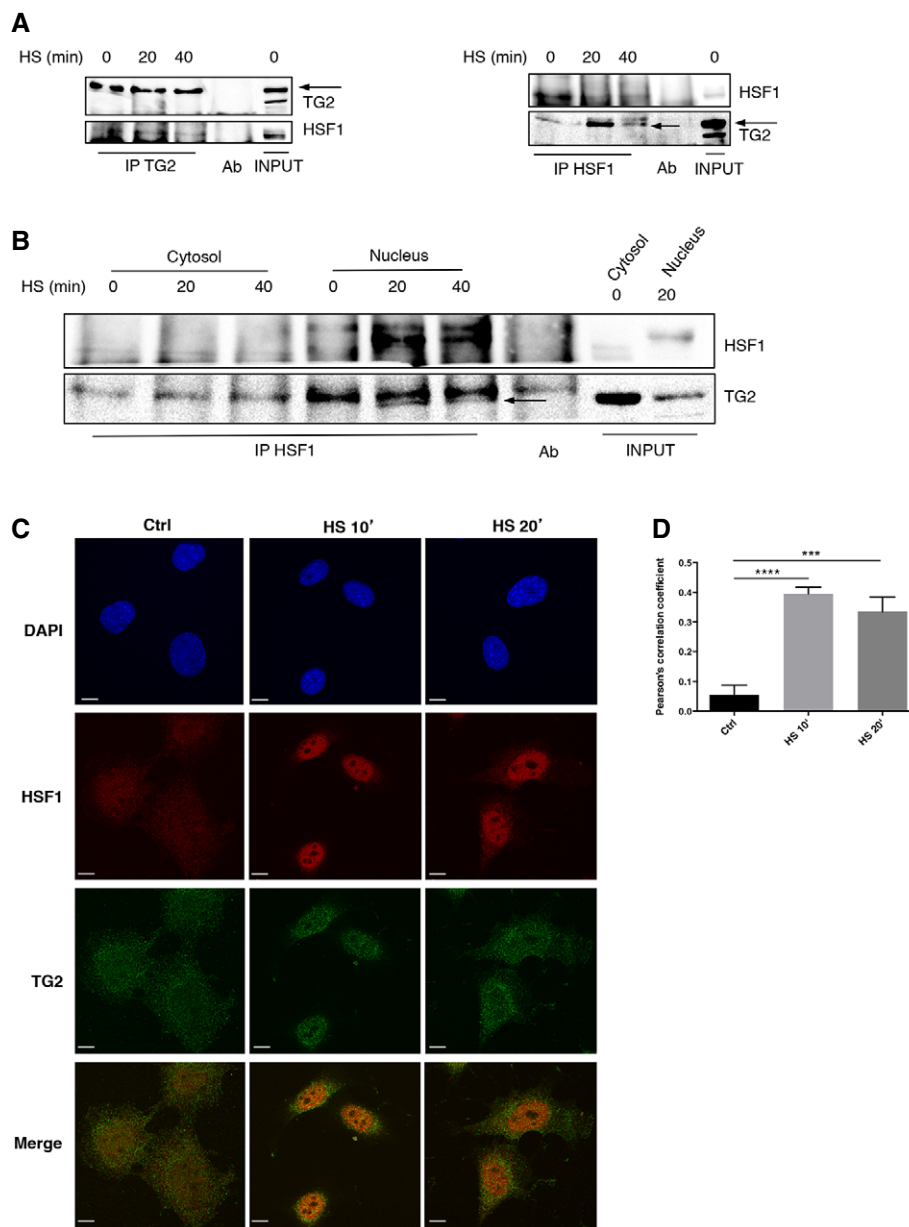
Figure 4. TG2 interacts with HSF1 in the nuclear compartment of cells exposed to heat shock.

A   TG2$^{-/-}$ MEF^{TG2} cell lysates were subjected to immunoprecipitation for TG2 (left) and HSF1 (right) upon heat shock for 20 and 40 min. Immuno- and co-immunoprecipitated proteins were separated by SDS–PAGE and blotted using the indicated antibodies. Whole-cell lysates (INPUT) were used as protein control.

B   Nuclear and cytosolic extracts, obtained from TG2$^{-/-}$ MEF^{TG2} exposed to heat shock for 20 and 40 min, were subjected to immunoprecipitation of HSF1. Immuno- and co-immunoprecipitated proteins were separated by SDS–PAGE and blotted using the indicated antibodies. Whole-cell lysates (INPUT) were used as protein control. The arrows indicate the TG2-specific band.

C   Immunofluorescence analysis of TG2 (green) and HSF1 (red) co-localization in TG2$^{+/+}$ MEF after exposure to thermal stress for 10 and 20 min. Scale bar 10 μm.

D   Histogram showing Pearson's correlation coefficient to evaluate co-localization of TG2 and HSF1.

Data information: Results are mean ± SEM; ***$P < 0.001$; ****$P < 0.0001$ (one-way ANOVA).

---

expression was increased in CFTR^{F508del}/TG2$^{+/+}$ mice over WT (CFTR^{wt}/TG2$^{+/+}$) controls, and this HSP70 overexpression was reduced in CFTR^{F508del}/TG2$^{-/-}$ mice (Fig 7A). Recently, it has been demonstrated that the administration of the TG2 inhibitor cysteamine restores CFTR function both in CF mice and patients bearing misfolded CFTR mutant proteins either in homozygous or in compound heterozygous form [17,23,24]. By a computerized docking analysis, we found that cysteamine was able to interact with TG2 close to its active site, thus inhibiting the transamidating and the PDI activities (Fig EV4A). In particular, the protonated amino group of cysteamine interacts with the triad His 335, Asp 358 and Glu 396 of TG2, thus being tightly bound to the enzyme. Moreover,
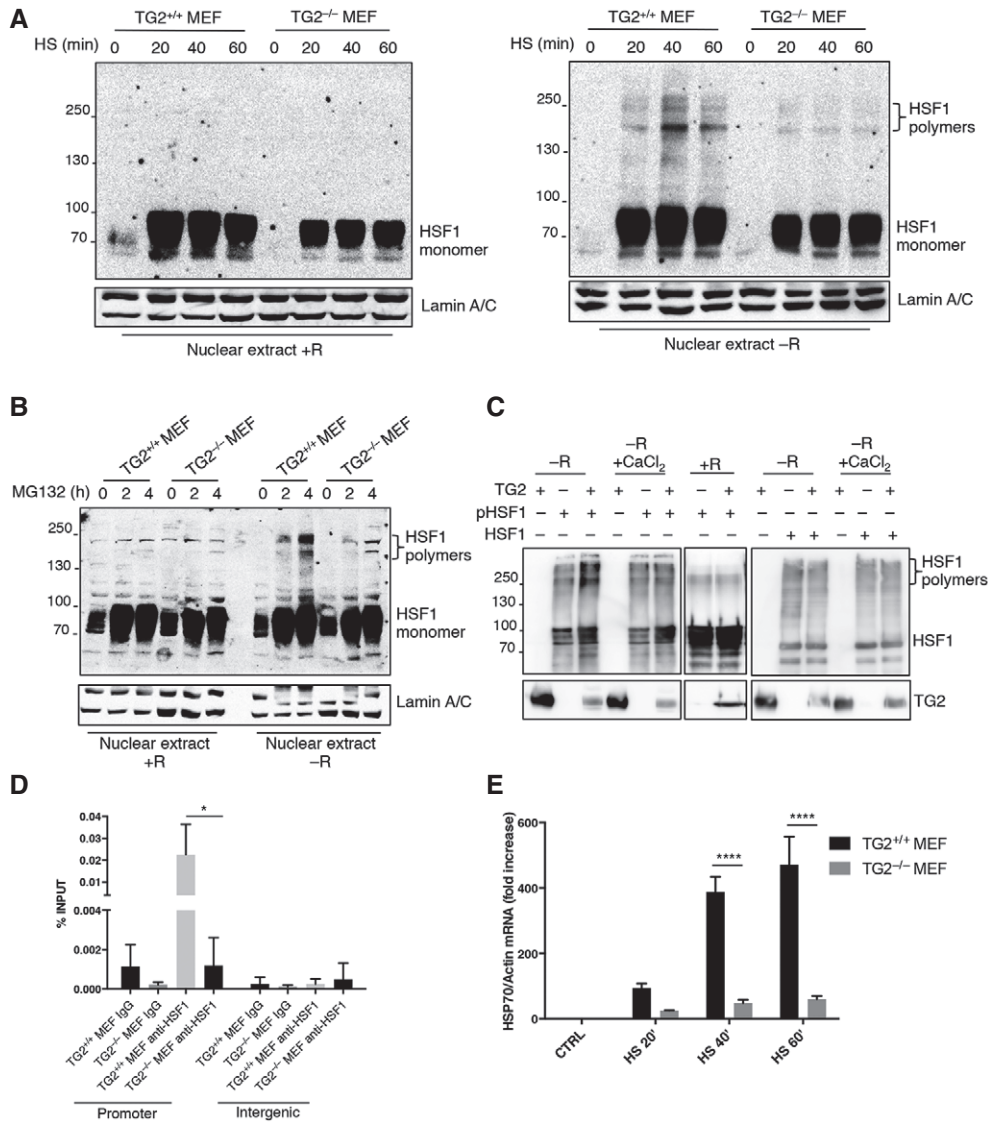
Figure 5. TG2 causes the trimerization and transcriptional activation of HSF1 by its PDI activity.

A, B   Western blot analysis of HSF1 in nuclear extracts of TG2$^{+/+}$ and TG2$^{-/-}$ MEFs after heat shock for 20, 40, 60 min (A) and proteasome inhibition treating with MG132 for 2 and 4 h (B). The analysis was performed in presence (+R) and absence (−R) of reducing agents to detect the formation of disulphide bonds. Lamin A/C was used as loading control.

C   Recombinant HSF1 or the phosphorylated isoform was incubated with recombinant TG2, in the presence or absence of calcium (CaCl$_2$) at 30°C for 1 h. The analysis was performed in presence (+R) and absence (−R) of reducing agents to detect the formation of disulphide bonds. The products of the *in vitro* assay were resolved by SDS–PAGE and blotted using the indicated antibodies.

D   ChIP-enriched DNA was prepared from TG2$^{+/+}$ and TG2$^{-/-}$ MEF treated with heat shock at 42°C for 10 min. ChIP-qPCR analysis was performed in the distal HSE (promoter) of HSP70 promoter and in intergenic regions, as negative control, using HSF1 antibody. ChIP signal of HSF1 was normalized as % of input. The *P*-value was determined by one-way ANOVA test followed by Tukey's post-test.

E   HSP70 mRNA levels, quantified by qPCR, in TG2$^{+/+}$ and TG2$^{-/-}$ MEF treated with heat shock at 42°C for 20, 40 and 60 min.

Data information: Results are mean ± SEM of three independent experiments; *$P < 0.05$; ****$P < 0.0001$ (one-way ANOVA).

this interaction drives the correct orientation of cysteamine with Cys 371, forming a covalent disulphide bridge. Notably, residue 371 is one of the cysteines involved in oxidative inactivation of TG2, through the formation of disulphide bonds [37]. These data indicate that the mechanism through which cysteamine inhibits TG2 could involve both the physical blockage of the active site and oxidative inactivation of the enzyme (Fig EV4A). Prompted by this evidence,

we decided to verify whether the TG2 inhibition by cysteamine could reduce HSP70 protein levels leading to its positive effects. We therefore analysed HSP70 expression in the intestine of CF mice (CFTR^{F508del}/TG2$^{+/+}$) after 5 days of oral administration with cysteamine (Fig 7B). Interestingly, cysteamine led to a significant reduction in HSP70 protein levels that returned to the levels observed in the wild-type mice (CFTR^{wt}/TG2$^{+/+}$). Next, to verify
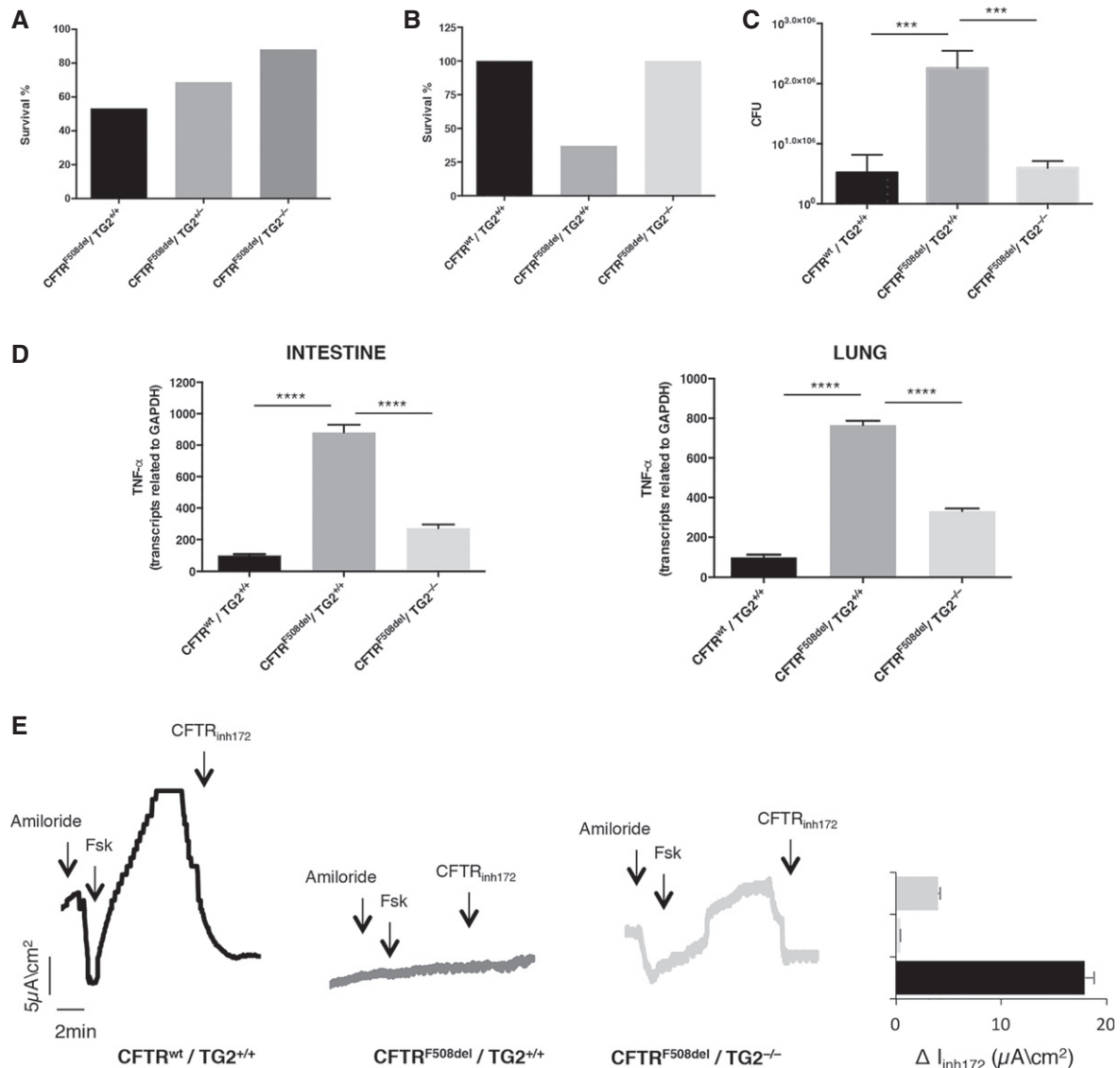
Figure 6. F508del CFTR function is restored in CF mice ablating TG2.

A   Survival rate of CFTR^{F508del}/TG2$^{-/-}$ ($n = 5/42$) and CFTR^{F508del}/TG2$^{+/-}$ ($n = 6/19$) mice compared to the CFTR^{F508del}/TG2$^{+/+}$ ($n = 7/15$) ones fed with a standard diet.
B   Survival rate of CFTR^{F508del}/TG2$^{-/-}$ mice ($n = 8/8$) compared to the CFTR^{F508del}/TG2$^{+/+}$ ones ($n = 3/8$) and the wild-type littermates (CFTR^{wt}/TG2$^{+/+}$)($n = 9/9$) after infection with PAO1 strain.
C   Number of colony-forming units (CFU) of CFTR^{F508del}/TG2$^{-/-}$ mice compared to the CFTR^{F508del}/TG2$^{+/+}$ ones and the wild-type littermates (CFTR^{wt}/TG2$^{+/+}$) after 24 h of infection with PAO1 strain of *Pseudomonas Aeruginosa*.
D   TNF-α transcription levels, quantified by qPCR, in intestine (left) and lung (right) homogenates from 10-week-old CFTR^{F508del}/TG2$^{-/-}$ ($n = 3$) and CFTR^{F508del}/TG2$^{+/+}$ ($n = 3$) mice.
E   Representative traces of CFTR-dependent Cl- secretion measured by forskolin (Fsk)-induced increase of chloride current (Isc (μA/cm^2)) in small intestines mounted in Ussing chambers; quantification of the peak CFTR inhibitor 172 (CFTRinh172)-sensitive Isc (ΔIsc) in tissue samples.

Data information: Results in (C–E) are mean ± SEM of three independent experiments; ***$P < 0.001$; ****$P < 0.0001$ (one-way ANOVA).

whether the TG2-HSF1-HSP70 axis was also detectable in CF patients homozygous for the F508del CFTR mutation, we examined HSP70 expression in primary nasal epithelial cells. *Ex vivo* treatment of freshly brushed patient cells with cysteamine significantly reduced the HSP70 protein levels observed in CF cells (Fig 7C). Cysteamine also decreased protein expression of HSP40 (Fig 7D) and HSP27 (Fig EV4B), others HSF1-regulated chaperones involved in F508del CFTR handling [42,43]. Moreover, we verified whether

the inhibition of TG2 by cysteamine could modulate HSP70 expression by interfering with its PDI activity. Notably, formation of HSF1 trimers in the nasal epithelial cells from CF patients was increased with respect to normal controls; however, cysteamine treatment abolished this increase (Fig 7E and F). According to this, phosphorylation of HSF1 at S326, a hallmark for HSF1 activation, occurred mainly in CF patients and largely decreased with cysteamine (Fig 7E and F). We also analysed freshly brushed nasal epithelial cells from

two F508del CFTR homozygous patients who underwent a phase II clinical trial (EudraCT 2013-001258-82) with cysteamine bitartrate [17]. Both patients, who showed functional rescue of mutant CFTR protein after 4 weeks of *in vivo* therapy [17], also manifested reduced HSP70 expression together with a decrease in TG2 protein (Fig EV4C). Altogether, our data indicate a pivotal role of TG2 in favouring F508del CFTR degradation through regulation of HSP70-HSF1 pathway. They also suggest that cysteamine can improve the rescue of a functional F508del CFTR by modulating the PDI activity of TG2 in the epithelial cells. Thus, cysteamine can exert pleiotropic effects, as it is capable of either avoiding TG2-mediated Ca^{2+}-dependent crosslinking of substrate proteins as well as of interfering with the activity of PDIs in CF epithelial cells.

Discussion

One of the mechanisms through which eukaryotic cells adapt to intracellular and environmental stress is the heat-shock response. The master transcription factor regulating this pathway is HSF1 that, by controlling a large set of target genes, allows the stressed cell to survive. Under normal conditions, monomeric HSF1 is localized in the cytoplasm bound to some HSPs (HSP70 and 90). Upon stress, HSF1 is released from these binding partners and trimerizes, forming a complex that translocates into the nucleus where it binds to DNA and activates target genes [30,31]. Our study demonstrates that TG2 plays a key upstream role in the regulation of proteostasis by catalysing the trimerization of HSF1. Here, we provide the first evidence that the HSF1 trimerization is mediated by the PDI activity of TG2 (Fig EV5). The formation of three intermolecular S-S bonds between two cysteine residues (Cys36 and Cys103) is essential for HSF1 trimerization and DNA binding [35]. However, so far the mechanism by which Cys36 and Cys103 form this intermolecular S-S bond was elusive. Here, we show that the PDI activity of TG2 catalyses HSF1 trimerization and its absence/inhibition impairs translocation of the HSF1 trimeric complex in the nucleus. In keeping with these evidences, mice lacking TG2 displayed a markedly impaired response to HS characterized by the absence of HSF1 trimer formation. In the absence of TG2, we also detected a marked difference in the HSF1 phosphorylation profile, largely proposed as a requirement for HSF-driven transcription [44], even if recent evidences show that the phosphorylation status of HSF1 does not affect the subcellular localization and DNA-binding activity of HSF1 [45]. Taken together, these findings demonstrate the key role played by TG2 in the control of cellular stress homeostasis via the post-translational modification of HSF1. Another aspect of the present study is that it clarifies and extends prior observations on the role of TG2 in degenerative disorders, such as the Huntington disease (HD), in which TG2 inhibitors such as cysteamine reversed transcriptional deregulation due to the expression of mutated huntingtin [46,47]. These studies showed that the treatment of HD cells with TG2 inhibitors resulted in a broad normalization of several hundred genes that are deregulated by the expression of the mutated huntingtin. Interestingly, among these TG2-sensitive genes, many are known to be also controlled by HSF1 [47]. It is important to note that, so far, no model was proposed to explain how the TG2 inhibition regulates transcription under proteomic stress, but based on the present study it is possible to suggest that TG2 might exert its

transcriptional function through modulation of HSF1 activity. In agreement with this novel function of TG2, it was previously described that stressed cells lacking TG2 are defective in the clearance of ubiquitinated protein aggregates thus predisposing them to death [12,48]. Indeed, the peculiar biochemistry of TG2, as well its capacity to interact with the major proteins involved in the regulation of proteostasis [18,48] in various intracellular compartments, confers to TG2 a unique ability to act as a guardian of the proteome under stressful conditions. In keeping with this assumption, recent evidence has highlighted a role for TG2 in the regulation of the main pathways controlling proteome homeostasis including autophagy, proteasomes and exosomes [4,11,13,14]. Likewise, HSF1 and the HSPs have been shown to play a key regulatory role in dictating the fate of their abnormal client proteins versus the proteasome and/or autophagy [31]. TG2 function/regulation has been implicated in the pathogenesis of several major human diseases, such as cancer and metastasis formation, cystic fibrosis, coeliac disease and neurodegenerative disorders [49]. Here, we focused our attention on CF, showing that the ablation/inhibition of TG2 significantly ameliorated the typical CF symptoms in a double-transgenic mouse model in which the F508del CFTR mutation was backcrossed into a TG2 null background. Interestingly, CFTR^{F508del} TG2$^{-/-}$ mice exhibited a partial recovery (about 40%) of the CFTR functionality and exhibited a marked amelioration of CF symptoms, including reduced inflammatory and pulmonary inflammation as well as improved clearance of, and resistance to, *Pseudomonas aeroginosa*. Importantly, restoring even < 30% of CFTR function *in vivo* is believed to confer a clinical benefit to CF patients [24]. In fact, rescuing approximately 20% of function of WT CFTR prevents the CF-associated intestinal manifestations in newborn F508del CFTR homozygous pigs [24]. Thus, even a partial rescue of CFTR function, as that elicited by the ablation of TG2, may explain the amelioration of the CF phenotype. The improvements observed in the absence of TG2 were paralleled by reduction in the HSF1 trimerization, resulting in a drastic reduction in HSP70 levels. It is important to note that similar findings were also detected in epithelial cells obtained from the nasal brushing of CF patients treated with the TG2 inhibitor cysteamine, which has been demonstrated to be clinically efficient in CF. Thus, systemic cysteamine treatment switches off inflammation, rescues F508del CFTR protein expression and restores its function at the PM, both in the lungs from CFTR^{F508del} TG2$^{+/+}$ mice and in F508del CFTR bronchial epithelial cells from CF patients [24]. Taken together, these data highlight a key upstream novel role played by TG2 and HSF1 as general regulators of proteostasis in the CF pathogenesis. Indeed, the results of this study uncover a new and unexpected paradigm: reduction in HSPs levels, in the course of the CF disease, results in decreased degradation of the CFTR, thus leading to a positive outcome. Indeed, immature F508del CFTR fails to mature, does not transit to the late secretory pathway [50] and is trapped in the ER where interacts with the cytosolic chaperones, such as HSP70, as well as with the ER chaperone calnexin [38,42,51,52]. Ultimately, F508del CFTR, retained in the ER, is ubiquitinated and retrotranslocated to the cytosol where it undergoes proteasomal degradation by the ER-associated degradation (ERAD) pathway [53–56]. In this regard, in the last years it has become clear that HSF1 is able to regulate not only cytosolic but also ER and mitochondria proteins [57–60], suggesting a possible interplay between HSF1 activation and ERAD pathway, involved in CFTR degradation.
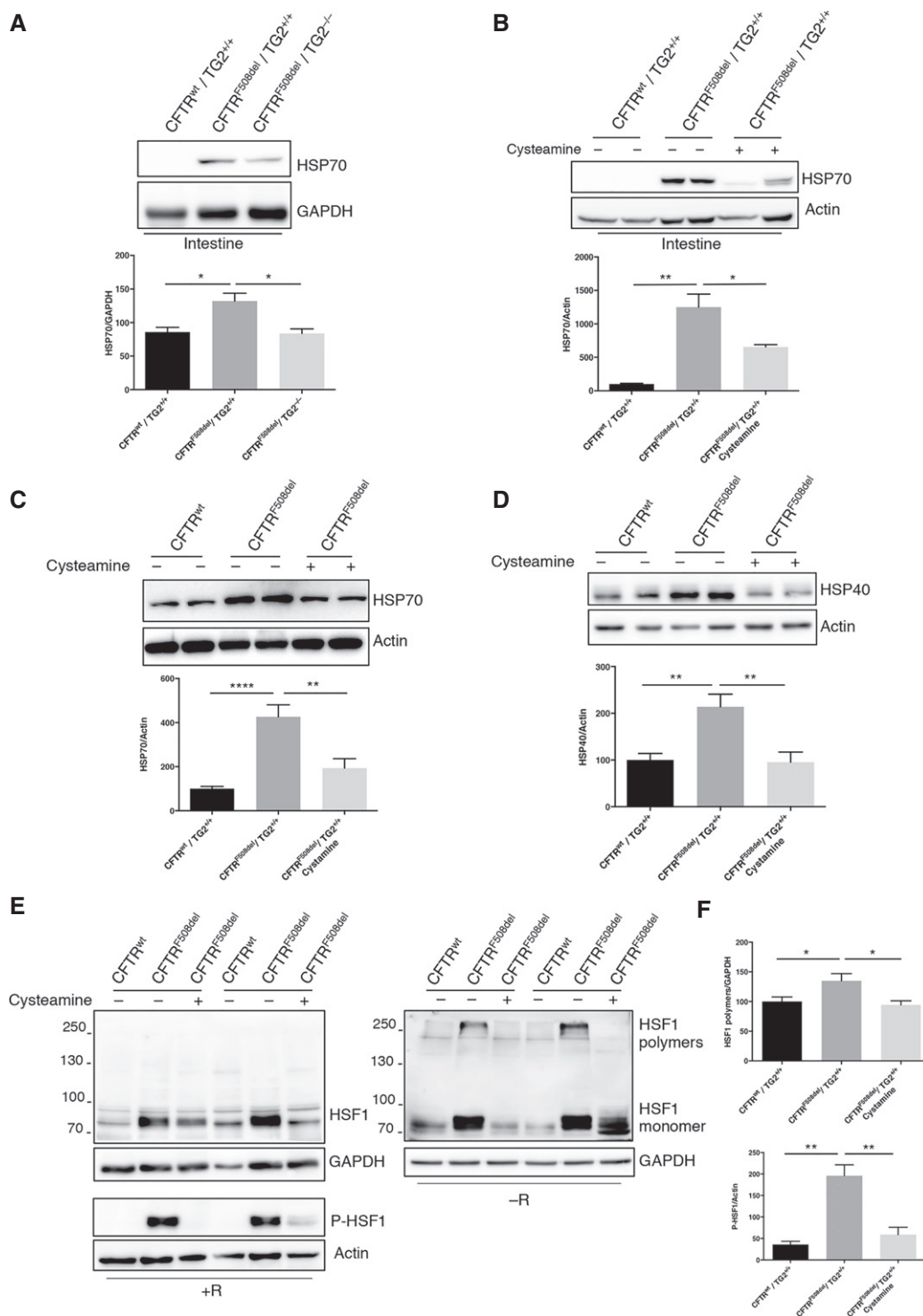
Figure 7. TG2 regulates HSF1 activity and HSP70 expression in CF.

A   Western blot analysis and densitometric analysis of HSP70 protein levels in the intestine tissue lysates of CFTR^F508del/TG2^−/− mice (*n* = 4) compared to the CFTR^F508del/TG2^+/+ ones (*n* = 4) and the wild-type littermates (CFTR^wt/TG2^+/+) (*n* = 4). GAPDH was used as loading control.

B   Western blot analysis and densitometric analysis of HSP70 protein levels in the intestine tissue lysates of CFTR^F508del/TG2^+/+ mice administrated with the TG2 inhibitor cysteamine (*n* = 3), compared to the untreated CFTR^F508del/TG2^+/+ ones (*n* = 3) and the wild-type littermates (CFTR^wt/TG2^+/+) (*n* = 3). Actin was used as loading control.

C, D Western blot and densitometric analysis of HSP70 and HSP40 protein levels in nasal epithelial cells, from CF patients (*n* = 6), cultured *ex vivo* with cysteamine for 18 h.

E   Western blot analysis of HSF1 and phosphorylated HSF1 at Ser326 in nasal epithelial cells, from CF patients (*n* = 6), cultured *ex vivo* with cysteamine for 18 h. The analysis was performed in presence (+R) and absence (−R) of reducing agents to detect the formation of disulphide bonds. GAPDH and Actin were used as loading control.

F   Densitometric analysis of HSF1 polymers formation and HSF1 phosphorylation in nasal epithelial cells, from CF patients, cultured *ex vivo* with cysteamine.

Data information: Results are mean ± SEM; *P < 0.05; **P < 0.01; ****P < 0.0001 (one-way ANOVA).

In addition, recent findings show that HSF1 is also able to regulate gene transcription for the maintenance of proteostasis capacity in unstressed conditions [61]. In fact, accumulating evidences show that HSF1 is activated in the nucleus as a consequence of diverse specific physiological cellular requirements and directs transcriptional programmes distinct from the heat-shock response.

In conclusion, our findings may open new perspectives in drug discovery programmes aimed at the identification of new inhibitors of PDIs to circumvent CFTR defect. Given the fact that cysteamine can inhibit the PDI activity of TG2 in a direct fashion, by a direct molecular interaction with the enzyme and its critical cysteines, it appears that most, if not all, of the cysteamine effects on CF must be considered as "on-target". It remains to be determined whether yet-to-be-developed specific TG2 PDI inhibitors may replace cysteamine advantageously for the treatment of CF or other diseases linked to TG2 deregulation.

Materials and Methods

Cell lines and drug treatments

$TG2^{+/+}$ and $TG2^{-/-}$ MEFs (murine embryonic fibroblasts) were obtained by spontaneous immortalization of fibroblasts derived from C57BL/6 mice embryos either wild type or knockout for TG2. $TG2^{-/-}$ MEF^{TG2} stably reconstituted with the unmutated TG2 was obtained as previously described [4]. To silence TG2, $TG2^{+/+}$ MEF was transfected with pLKO.1 plasmid (Sigma) containing an shRNA insert specific for TG2 (shTG2) or an shRNA insert that does not target any known genes from any species (no target shRNA). Transfection was performed using Lipofectamine 2000 (Invitrogen) according to the manufacturer's instructions, and the cells were selected for puromycin (Sigma) resistance using the antibiotic added to the culture medium (2 μg/ml). MEF cells were cultured in Dulbecco's modified Eagle's medium (Lonza) supplemented with 10% foetal bovine serum, 100 μg/ml streptomycin and 100 units/ml penicillin, at 37°C and 5% CO_2 in a humidified atmosphere. To induce heat shock, cells were placed in a water bath at 42°C followed, where indicated, by recovery to 37°C. To block proteasome activity, cells were incubated in full medium in the presence of 5 μM MG132 (Z-Leu-Leu-Leu-al, Sigma-Aldrich) for the indicated time. TG2 transamidating activity was inhibited incubating the cells with 40 μM Z-DON (Zedira). Nasal epithelial cells were collected by nasal brushing from two F508del CFTR homozygous CF patients enrolled in a previous open-label phase II clinical trial (EudraCT number #2013-001258-82 approved by Local Ethics Committee, Protocol reference #85/13) at the Regional Cystic Fibrosis Care Center, University of Naples Federico II A. All patients gave written informed consent at the time of the clinical study. The patients were treated as described [17,24], and nasal cells were collected previously and after 8 weeks of treatment with cysteamine. After nostril washing to remove mucus, cytological brushes (Robimpex, MO11157) were used to scrape the mid part of the inferior turbinate from both nasal nostrils. Brushes with cells were immediately transferred into RPMI 1640 medium (Invitrogen) containing 1% penicillin–streptomycin (Lonza), in 15-ml sterilized tubes. The tubes were incubated at 37°C for 2 h on a thermoshaker, to remove all cells from brushes, the brushes were

then removed, and the cells were centrifuged at $800 \times g$ for 20 min. The supernatant fractions were discarded and the cell pellet treated with 150 μl of trypsin–versene (EDTA) solution (Lonza) for 4 min at 37°C to disaggregate possible cell clusters. Trypsin solution was inactivated by adding 3 ml of serum-free bronchial epithelial cell growth medium BEGM (Clonetics, Lonza). After centrifugation at $800 \times g$ for 10 min, cells were plated with 10 ml of BEGM medium. Non-specific epithelial cells were removed during the daily cell washing and medium changes. Counterstaining with specific antibody was used to exclude the presence of lymphocytes, inflammatory cells and mucipar differentiation. For *ex vivo* treatments, the cells were incubated with or without cysteamine (250 μM) for 18 h.

Generation of CFTR^{F508del}/TG2$^{-/-}$ mice

In order to obtain $TG2^{-/-}$ mice carrying F508del mutation in CFTR, C57Bl/6 knockout mice for TG2 [62] (obtained from Gerry Melino, Department of Experimental Medicine and Biochemical Sciences, University of Rome "Tor Vergata", Rome, Italy) were crossed with 129/FVB mice heterozygous for F508del mutation (obtained from Bob Scholte, Erasmus Medical Centre Rotterdam, the Netherlands, CF coordinated action programme EU FP6 LSHM-CT-2005-018932). TG2 genotype was assessed by PCR using primers:

5′-TCCTGACCTGAGTCCTCGTC-3′

5′-TACTCCAGCTTCTCGTTCTG-3′

5′-ACGAGACTAGTGAGACGTGC-3′, following the conditions 95°C for 5 min, then 35 cycles at 94°C for 1 min + 56°C for 45 s + 72°C for 1 min and then 72°C for 5 min, as previously described [62]. To assess the presence of F508del mutation, DNA was digested with SspI restriction enzyme (Thermo Scientific) at 37°C and PCR was carried out with primers:

5′-GGACGCAAAGAAAGGGATAAG-3′

5′-CACAACACTGACACAAGTAGC-3′, following the conditions 95°C for 5 min, then 33 cycles at 95°C for 1 min + 52°C for 1 min + 72°C for 1 min and then 72°C for 7 min.

After weaning, mice were fed with a standard diet and survival rate was evaluated in the 4 weeks following.

Animal treatments

To induce an hyperthermic stress in mice, an empty mouse cage and a tray filled with water were placed in an oven at least 2 h at 42°C. These conditions should provide a relative humidity of 75%, which favours efficient HS [63,64]. Eight-week-old mice were placed in the cage for 20 min at 42°C, after which they were transferred to a clean cage at room temperature. Cysteamine administration was performed in CFTR^{F508del} mice via gavage with cysteamine (60 mg/kg in 100 ml saline/day) or 100 ml saline/day for 5 consecutive day/week for 5 weeks. *P. aeruginosa* (PAO1) infection was performed in 6-week-old mice by intratracheal injection of 5×10^6 cell/mice for 24 h. At the end of the treatment, mice were anesthetized with avertin (tribromoethanol, 250 mg/kg, Sigma) and killed and lungs were collected for analysis. The whole lung of each mouse was homogenized in 1 ml of sterile 0.9% saline and 100 μl of appropriately serial diluted lung homogenates samples was plated in agar Petri dish in the presence of carbenicillin (100 μg/ml, Sigma) overnight at 37°C. Colony factor unit was

enumerated 24 h later [65,66]. All the procedures in mice were approved by the Local Ethics Committee for Animal Welfare (IACUC No. 713) and were carried out in strict respect of European and National regulations.

Western blot analysis

Tissues were lysed in 50 mM Tris–HCl pH 7.5, 50 mM NaCl, 320 mM sucrose, 1% Triton X-100, 10% glycerol supplemented with protease and phosphatase inhibitor cocktail. Cells were rinsed in ice-cold phosphate-buffered saline (PBS) and collected in lysis buffer containing 20 mM Tris–HCl pH 7.4, 150 mM NaCl and 1% Triton X-100 with protease inhibitor cocktail. Nuclear and cytosolic extracts were obtained using the NE-PER Nuclear and Cytoplasmic Extraction Kit (Thermo Scientific). Protein concentrations were determined by the Bradford assay, using bovine serum albumin as a standard. Aliquots of total protein extracts from cells and tissues after different treatments were resolved on SDS–polyacrylamide gel and transferred to a nitrocellulose membrane. Blots were blocked in 5% non-fat dry milk in T-PBS (PBS + 0.05% Tween-20) for 1 h at room temperature and then incubated overnight with the described antibodies. The membranes were incubated with HRP-conjugated secondary antibody for 1 h at room temperature, and the signal was detected by Immun-Star WesternC Kit (Bio-Rad Laboratories).

Immunoprecipitation

Cells were lysed in a buffer containing 150 mM NaCl, 50 mM Tris–HCl pH 7.5, 2 mM EDTA, 2% NP-40 and freshly added protease inhibitor cocktail. An amount of 1.5 mg of proteins from cell lysates were subjected to immunoprecipitation using 2 μg of specific antibodies in combination with 80 μl of Protein G PLUS-Agarose beads (Santa Cruz), overnight at 4°C. LDS Sample Buffer 4× (Life Technologies) containing 2.86 M 2-mercaptoethanol (Sigma-Aldrich) was added to beads, and samples were boiled at 95°C for 10 min. Supernatants were analysed by Western blot.

Fluorescence microscopy

TG2$^{+/+}$ MEF, grown on coverslips, were subjected to heat shock, then washed with PBS and fixed in 4% paraformaldehyde for 10 min at room temperature. Fixed cells were permeabilized with 0.1% Triton X-100 in PBS for 10 min, blocked with 3% BSA in PBS for 20 min and incubated with anti-TG2 and anti-HSF1 primary antibodies for 1 h. After washing, cells were incubated with Alexa Fluor 488-conjugated and Alexa Fluor 594-conjugated secondary antibodies. The coverslips were mounted on microscope slides, sealed with an antifade solution and examined under a Leica TCS SP5 confocal microscope equipped with an ×40 (NA 1.25) or ×63 (NA 1.4) oil-immersion objective (Deerfield, IL, USA). Quantification of co-localization was performed on six sets of images acquired with the same optical settings and excluding the consideration of autofluorescence. To determine fluorescent signal co-localization between different channels, the Coloc module of ImageJ was used. A median filter was applied to the images to reduce the background noise before threshold analysis. The degree of channels co-localization was analysed by considering the Pearson's coefficient.

In vitro assay of HSF1 polymerization

Recombinant His-TG2 (0.25 μg, Zedira) was incubated either with recombinant His-HSF1 (0.5 μg, Enzo) or with the phosphorylated His-HSF1 recombinant protein (0.5 μg, Enzo) in reaction buffer including 50 mM Tris–HCl pH 7.5, 150 mM NaCl, 10% glycerol in presence or not of 5 mM CaCl$_2$ for 1 h at 30°C. The reaction products were than denatured with LDS Sample Buffer 4× containing (+R) or not (−R) 2-mercaptoethanol, heated 10 min at 70°C and directly analysed by Western blotting.

Chromatin Immunoprecipitation assay

Chromatin Immunoprecipitation was performed as previously described [67]. TG2$^{+/+}$ and TG2$^{-/-}$ MEFs, exposed to heat shock, were crosslinked in 1% (vol/vol) formaldehyde for 10 min at room temperature and quenched with 125 mM glycine for 5 min. Then, cells were washed twice with PBS, scraped and pelleted by centrifugation at 1,300 × g for 10 min and stored at 80°C until further use. Cells were lysed with a mild lysis buffer, and nuclei were enriched by centrifugation at 14,000 × g for 10 min. Nuclei were lysed with a nuclear lysis buffer and chromatin was sheared by sonication (Diagenode, Belgium, 30-s pulses, 30-s rests) on ice. Successful fragmentation was confirmed on a 0.8% agarose gel electrophoresis by comparing to unsheared chromatin. Immunoprecipitation was only done when sheared DNA had a size between 100 and 1,000 bp. Sheared chromatin was diluted in ChIP dilution buffer, and 100 μg was immunoprecipitated with magnetic protein G beads and 3 μg of primary antibody (α-HSF-1, Millipore ABE1044) overnight at 4°C by head-to-head rotation. The precipitated material was washed subsequently with a low salt buffer, high salt buffer and Tris–EDTA buffer for 5 min each with head-to-head rotation. The precipitated material was also treated with RNAse R at 37°C for 15 min and with 0.5 mg/ml Proteinase K at 50°C for 1 h to remove all contaminating RNA molecules and proteins. Eluted DNA was purified and subjected to qPCR analysis with primers directed against the HSP70.3 promoter region (mHSP70.3 dHSE Fwd 5′-ACCCTCCCCCT CAGGAATC-3′; mHSP70.3 dHSE Rev 5′-TGTCCAGAACTCTCCAG AGGTTT-3′). A primer set amplifying an HSP70.3 intergenic region (mHSP70.3 Intergenic Region Fwd 5′-GTGGCGCATGCCTTTGAT-3′; mHSP70.3 Intergenic Region Rev 5′-CTTTGTAGAACAGGCTGAC CTTGA-3′) was used as control for the ChIP.

Ussing chamber

CFTR-dependent chloride secretion was measured *ex vivo* in segment of mice ileum mounted in Ussing chambers. Chambers were obtained from Physiologic Instruments (model P2300, San Diego, CA, USA). Chamber solution was buffered by bubbling with a mixture of 95% O$_2$ and 5% CO$_2$. Tissues were short-circuited using Ag/AgCl agar electrodes. Short-circuit current and resistance were acquired or calculated using the VCC-600 transepithelial clamp from Physiologic Instruments and the Acquire &Analyze2•3 software for data acquisition (Physiologic Instruments), as previously described [17]. A basolateral-to-apical chloride gradient was established by replacing NaCl with Na-gluconate in the apical (luminal) compartment to create a driving force for CFTR-dependent Cl$^-$ secretion. CFTR channels present at the apical surface of the

epithelium (lumen side of the tissue) were activated. Stimulations with forskolin, CFTR inhibitor 172 and amiloride were performed as described [17].

RNA isolation and qPCR

Total RNA from MEF cells was extracted using Trizol reagent (Invitrogen, Carlsbad, CA) according to the manufacturer's instructions and then treated with Dnase I to remove contaminant DNA. Total RNA from mouse lung and intestine homogenates was extracted with the Pure Link RNA Mini Kit (Ambion, Life Technologies). 2 μg of RNA was retro-transcribed using AMV RT reverse transcriptase (Promega) and used in quantitative RT–PCR (qPCR) experiment, using SYBR green Supermix (BIO-RAD) following manufacturer's instructions. Thermocycling consisted of an initial polymerase activation step at 98°C for 5 min, and amplification was performed with 35 cycles of 95°C for 15 s, 68°C for 10 s and 72°C for 20 s with data acquisition at this stage and the reaction finished by the built-in melt curve. The relative amounts of mRNA were calculated by using the comparative Ctmethod. HSP70 primers: 5′-ATGGACAAGGCGCA GATCC-3′, 5′-CTCCGACTTGTCCCCCAT-3′. Actin primers: 5′-GGC TGTATTCCCCTCCATCG-3′, 5′-CCAGTTGGTAACAATGCCATGT-3′. TNFα primers: 5′-CCACCACGCT CTTCTGTCTA-3′ and 5′-AGGGT CTGGGCCATAGAACT-3′.

Computerized docking analyses

TG2 crystal structure was retrieved from the protein data bank (PDB code: 3S3J) and processed in order to remove unwanted ligands and water molecules. Hydrogen atoms were added to the protein structure using standard geometries. To minimize contacts between hydrogens, the structure was subjected to Amber99 force-field minimization until the rms (root-mean-square) of conjugate gradient was <0.1 kcal/mol/Å (1Å = 0.1 nm) keeping the heavy atoms fixed at their crystallographic positions [68]. After protein preparation, a site finder approach was used to retrieve information about all the possible interaction sites suitable with cysteamine size and chemical properties. Only one binding site, defined by His 335, Asp 358, Cys 371, Phe 392 and Glu 396, resulted to be compatible and was then selected for the docking analysis. The docking procedure was performed using AUTODOCK software [69].

Statistical analysis

GraphPad was used for statistical analysis. ImageJ64 software was used for densitometric analysis. Statistical significance was determined using the Student's *t*-test or one-way ANOVA test. *P*-value smaller than 0.05 ($P < 0.05$) was considered to be significant.

Expanded View for this article is available online.

Author contributions

FR designed and performed most of the experiments. VRV and SE processed the human samples from CF patients. MD and MGF produced MEF cells and along with LO who helped with the experiments. EF, RM and NAB performed the experiments on CF mice. VP and CS planned and performed the CHIP assay. GC performed the bioinformatics analysis. LF performed the immunofluorescence analysis. GMF and GK analysed all data. VR provided the human samples from CF patients. MP and LM conceived the project and designed the experiments. MP, FR and LM wrote the manuscript. All authors read and edited the manuscript.

Conflict of interest

The authors declare that they have no conflict of interest.

References

1. Fesus L, Piacentini M (2002) Transglutaminase 2: an enigmatic enzyme with diverse functions. *Trends Biochem Sci* 27: 534 – 539
2. Lorand L, Graham RM (2003) Transglutaminases: crosslinking enzymes with pleiotropic functions. *Nat Rev Mol Cell Biol* 4: 140 – 156
3. Nurminskaya MV, Belkin AM (2012) Cellular functions of tissue transglutaminase. *Int Rev Cell Mol Biol* 294: 1 – 97
4. Rossin F, D'Eletto M, Macdonald D, Farrace MG, Piacentini M (2012) TG2 transamidating activity acts as a reostat controlling the interplay between apoptosis and autophagy. *Amino Acids* 42: 1793 – 1802
5. Mastroberardino PG, Farrace MG, Viti I, Pavone F, Fimia GM, Melino G, Rodolfo C, Piacentini M (2006) "Tissue" transglutaminase contributes to the formation of disulphide bridges in proteins of mitochondrial respiratory complexes. *Biochim Biophys Acta* 1757: 1357 – 1365
6. Gundemir S, Colak G, Tucholski J, Johnson GVW (2012) Transglutaminase 2: a molecular swiss army knife. *Biochim Biophys Acta* 1823: 406 – 419
7. Altuntas S, Rossin F, Marsella C, D'Eletto M, Diaz-Hidalgo L, Farrace MG, Campanella M, Antonioli M, Fimia GM, Piacentini M (2015) The transglutaminase type 2 and pyruvate kinase isoenzyme M2 interplay in autophagy regulation. *Oncotarget* 6: 44941 – 44954
8. Caccamo D, Condello S, Ferlazzo N, Currò M, Griffin M, Ientile R (2013) Transglutaminase 2 interaction with small heat shock proteins mediate cell survival upon excitotoxic stress. *Amino Acids* 44: 151 – 159
9. Ergulen E, Bécsi B, Csomós I, Fésüs L, Kanchan K (2016) Identification of DNAJA1 as a novel interacting partner and substrate of human transglutaminase 2. *Biochem J* 473: 3889 – 3901
10. Min B, Park H, Lee S, Li Y, Choi JM, Lee JY, Kim J, Choi YD, Kwon YG, Lee HW *et al* (2016) CHIP-mediated degradation of transglutaminase 2 negatively regulates tumor growth and angiogenesis in renal cancer. *Oncogene* 35: 3718 – 3728

11. D'Eletto M, Farrace MG, Falasca L, Reali V, Oliverio S, Melino G, Griffin M, Fimia GM, Piacentini M (2009) Transglutaminase 2 is involved in autophagosome maturation. *Autophagy* 5: 1145–1154

12. D'Eletto M, Farrace MG, Rossin F, Strappazzon F, Giacomo GD, Cecconi F, Melino G, Sepe S, Moreno S, Fimia GM *et al* (2012) Type 2 transglutaminase is involved in the autophagy-dependent clearance of ubiquitinated proteins. *Cell Death Differ* 19: 1228–1238

13. Rossin F, D'Eletto M, Falasca L, Sepe S, Cocco S, Fimia GM, Campanella M, Mastroberardino PG, Farrace MG, Piacentini M (2015) Transglutaminase 2 ablation leads to mitophagy impairment associated with a metabolic shift towards aerobic glycolysis. *Cell Death Differ* 22: 408–418

14. Diaz-Hidalgo L, Altuntas S, Rossin F, D'Eletto M, Marsella C, Farrace MG, Falasca L, Antonioli M, Fimia GM, Piacentini M (2016) Transglutaminase type 2-dependent selective recruitment of proteins into exosomes under stressful cellular conditions. *Biochim Biophys Acta* 1863: 2084–2092

15. Van Raamsdonk JM, Pearson J, Bailey CD, Rogers DA, Johnson GV, Hayden MR, Leavitt BR (2005) Cystamine treatment is neuroprotective in the YAC128 mouse model of Huntington disease. *J Neurochem* 95: 210–220

16. Dohil R, Meyer L, Schmeltzer S, Cabrera BL, Lavine JE, Phillips SA (2012) The effect of cysteamine bitartrate on adiponectin multimerization in non-alcoholic fatty liver disease and healthy subjects. *J Pediatr* 161: 639–645

17. Tosco A, De Gregorio F, Esposito S, De Stefano D, Sana I, Ferrari E, Sepe A, Salvadori L, Buonpensiero P, Di Pasqua A *et al* (2016) A novel treatment of cystic fibrosis acting on-target: cysteamine plus epigallocatechin gallate for the autophagy-dependent rescue of class II-mutated CFTR. *Cell Death Differ* 23: 1380–1393

18. Altuntas S, D'Eletto M, Rossin F, Hidalgo LD, Farrace MG, Falasca L, Piredda L, Cocco S, Mastroberardino PG, Piacentini M *et al* (2014) Type 2 transglutaminase, mitochondria and Huntington's disease: menage a trois. *Mitochondrion* 19: 97–104

19. Piacentini M, D'Eletto M, Farrace MG, Rodolfo C, Del Nonno F, Ippolito G, Falasca L (2014) Characterization of distinct sub-cellular location of transglutaminase type II: changes in intracellular distribution in physiological and pathological states. *Cell Tissue Res* 358: 793–805

20. Siegel M, Khosla C (2007) Transglutaminase 2 inhibitors and their therapeutic role in disease states. *Pharmacol Ther* 115: 232–245

21. Bousquet M, Gibrat C, Ouellet M, Rouillard C, Calon F, Cicchetti F (2010) Cystamine metabolism and brain transport properties: clinical implications for neurodegenerative diseases. *J Neurochem* 114: 1651–1658

22. Anderson MP, Sheppard DN, Berger HA, Welsh MJ (1992) Chloride channels in the apical membrane of normal and cystic fibrosis airway and intestinal epithelia. *Am J Physiol* 263: L1–L14

23. Luciani A, Villella VR, Esposito S, Brunetti-Pierri N, Medina D, Settembre C, Gavina M, Pulze L, Giardino I, Pettoello-Mantovani M *et al* (2010) Defective CFTR induces aggresome formation and lung inflammation in cystic fibrosis through ROS-mediated autophagy inhibition. *Nat Cell Biol* 12: 863–875

24. De Stefano D, Villella VR, Esposito S, Tosco A, Sepe A, Gregorio FD, Salvadori L, Grassia R, Leone CA, Rosa GD *et al* (2014) Restoration of CFTR function in patients with cystic fibrosis carrying the F508del-CFTR mutation. *Autophagy* 10: 2053–2074

25. Esposito S, Tosco A, Villella VR, Raia V, Kroemer G, Maiuri L (2016) Manipulating proteostasis to repair the F508del-CFTR defect in cystic fibrosis. *Mol Cell Pediatr* 3: 13.

26. Xia W, Voellmy R (1997) Hyperphosphorylation of heat shock transcription factor 1 is correlated with transcriptional competence and slow dissociation of active factor trimers. *J Biol Chem* 272: 4094–4102

27. Du ZX, Zhang HY, Meng X, Gao YY, Zou RL, Liu BQ, Guan Y, Wang HQ (2009) Proteasome inhibitor MG132 induces BAG3 expression through activation of heat shock factor 1. *J Cell Physiol* 218: 631–637

28. Qi W, White MC, Choi W, Guo C, Dinney C, McConkey DJ, Siefker-Radtke A (2013) Inhibition of inducible heat shock protein-70 (hsp72) enhances bortezomib-induced cell death in human bladder cancer cells. *PLoS One* 8: e69509

29. Morimoto RI (1998) Regulation of the heat shock transcriptional response: cross talk between a family of heat shock factors, molecular chaperones, and negative regulators. *Genes Dev* 12: 3788–3796

30. Åkerfelt M, Morimoto RI, Sistonen L (2010) Heat shock factors: integrators of cell stress, development and lifespan. *Nat Rev Mol Cell Biol* 11: 545–555

31. Calderwood SK, Xie Y, Wang X, Khaleque MA, Chou SD, Murshid A, Prince T, Zhang Y (2010) Signal transduction pathways leading to heat shock transcription. *Sign Transduct Insights* 2: 13–24

32. Baler R, Dahl G, Voellmy R (1993) Activation of human heat shock genes is accompanied by oligomerization, modification, and rapid translocation of heat shock transcription factor HSF1. *Mol Cell Biol* 13: 2486–2496

33. Pirkkala L, Nykänen P, Sistonen L (2001) Roles of the heat shock transcription factors in regulation of the heat shock response and beyond. *FASEB J* 15: 1118–1131

34. Jin YH, Ahn SG, Kim SA (2015) BAG3 affects the nucleocytoplasmic shuttling of HSF1 upon heat stress. *Biochem Biophys Res Commun* 464: 561–567

35. Ahn SG, Thiele DJ (2003) Redox regulation of mammalian heat shock factor 1 is essential for Hsp gene activation and protection from stress. *Genes Dev* 17: 516–528

36. Lu M, Kim HE, Li CR, Kim S, Kwak IJ, Lee YJ, Kim SS, Moon JY, Kim CH, Kim DK *et al* (2008) Two distinct disulfide bonds formed in human heat shock transcription factor 1 act in opposition to regulate its DNA binding activity. *Biochemistry* 47: 6007–6015

37. Stamnaes J, Pinkas DM, Fleckenstein B, Khosla C, Sollid LM (2010) Redox regulation of transglutaminase 2 activity. *J Biol Chem* 285: 25402–25409

38. Yang Y, Janich S, Cohn J, Wilson JM (1993) The common variant of cystic fibrosis transmembrane conductance regulator is recognized by hsp70 and degraded in a pre-Golgi non lysosomal compartment. *Proc Natl Acad Sci USA* 90: 9480–9484

39. Kopito RR (1999) Biosynthesis and degradation of CFTR. *Physiol Rev* 79: 167–173

40. Roberts RG (2014) Living in constant crisis–when stress management becomes the problem. *PLoS Biol* 12: e1001999

41. Roth DM, Hutt DM, Tong J, Bouchecareilh M, Wang N, Seeley T, Dekkers JF, Beekman JM, Garza D, Drew L *et al* (2014) Modulation of the maladaptive stress response to manage diseases of protein folding. *PLoS Biol* 12: e1001998

42. Meacham GC, Lu Z, King S, Sorscher E, Tousson A, Cyr DM (1999) The Hdj-2/Hsc70 chaperone pair facilitates early steps in CFTR biogenesis. *EMBO J* 18: 1492–1505

43. Ahner A, Gong X, Schmidt BZ, Peters KW, Rabeh WM, Thibodeau PH, Lukacs L, Frizzell RA (2013) Small heat shock proteins target mutant cystic fibrosis transmembrane conductance regulator for degradation via a small ubiquitin-like modifier-dependent pathway. *Mol Biol Cell* 24: 74–84

44. Chou SD, Prince T, Gong J, Calderwood SK (2012) mTOR is essential for the proteotoxic stress response, HSF1 activation and heat shock protein synthesis. *PLoS One* 7: e39679

45. Budzyński MA, Puustinen MC, Joutsen J, Sistonen L (2015) Uncoupling stress-inducible phosphorylation of heat shock factor 1 from its activation. *Mol Cell Biol* 35: 2530–2540

46. Mastroberardino PG, Piacentini M (2010) Type 2 transglutaminase in Huntington's disease: a double-edged sword with clinical potential. *J Intern Med* 268: 419–431

47. McConoughey SJ, Basso M, Niatsetskaya ZV, Sleiman SF, Smirnova NA, Langley BC, Mahishi L, Cooper AJ, Antonyak MA, Cerione RA *et al* (2010) Inhibition of transglutaminase 2 mitigates transcriptional dysregulation in models of Huntington disease. *EMBO Mol Med* 2: 349–370

48. Rossin F, D'Eletto M, Farrace MG, Piacentini M (2014) Transglutaminase type 2: a multifunctional protein chaperone? *Mol Cell Oncol* 1: e968506

49. Iismaa SE, Mearns BM, Lorand L, Graham RM (2009) Transglutaminases and disease: lessons from genetically engineered mouse models and inherited disorders. *Physiol Rev* 89: 991–1023

50. Lukacs GL, Mohamed A, Kartner N, Chang XB, Riordan JR, Grinstein S (1994) Conformational maturation of CFTR but not its mutant counterpart (delta F508) occurs in the endoplasmic reticulum and requires ATP. *EMBO J* 13: 6076–6086

51. Pind S, Riordan JR, Williams DB (1994) Participation of the endoplasmic reticulum chaperone calnexin (p88, IP90) in the biogenesis of the cystic fibrosis transmembrane conductance regulator. *J Biol Chem* 269: 12784–12788

52. Loo MA, Jensen TJ, Cui L, Hou Y, Chang XB, Riordan JR (1998) Perturbation of Hsp90 interaction with nascent CFTR prevents its maturation and accelerates its degradation by the proteasome. *EMBO J* 17: 6879–6887

53. Jensen TJ, Loo MA, Pind S, Williams DB, Goldberg AL, Riordan JR (1995) Multiple proteolytic systems, including the proteasome, contribute to CFTR processing. *Cell* 83: 129–135

54. Knittler MR, Dirks S, Haas IG (1995) Molecular chaperones involved in protein degradation in the endoplasmic reticulum: quantitative interaction of the heat shock cognate protein BiP with partially folded immunoglobulin light chains that are degraded in the endoplasmic reticulum. *Proc Natl Acad Sci USA* 92: 1764–1768

55. Johnston JA, Ward CL, Kopito RR (1998) Aggresomes: a cellular response to misfolded proteins. *J Cell Biol* 143: 1883–1898

56. Gelman MS, Kannegaard ES, Kopito RR (2002) A principal role for the proteasome in endoplasmic reticulum-associated degradation of misfolded intracellular cystic fibrosis transmembrane conductance regulator. *J Biol Chem* 277: 11709–11714

57. Takemori Y, Sakaguchi A, Matsuda S, Mizukami Y, Sakurai H (2006) Stress-induced transcription of the endoplasmic reticulum oxidoreductin gene ERO1 in the yeast Saccharomyces cerevisiae. *Mol Genet Genomics* 275: 89–96

58. Sakurai H, Ota A (2011) Regulation of chaperone gene expression by heat shock transcription factor in Saccharomyces cerevisiae: importance in normal cell growth, stress resistance, and longevity. *FEBS Lett* 585: 2744–2748

59. Heldens L, Hensen SM, Onnekink C, van Genesen ST, Dirks RP, Lubsen NH (2011) An atypical unfolded protein response in heat shocked cells. *PLoS One* 6: e23512

60. Kim E, Sakata K, Liao FF (2017) Bidirectional interplay of HSF1 degradation and UPR activation promotes tau hyperphosphorylation. *PLoS Genet* 13: e1006849

61. Fujimoto M, Nakai A (2010) The heat shock factor family and adaptation to proteotoxic stress. *FEBS J* 277: 4112–4125

62. De Laurenzi V, Melino G (2001) Gene disruption of tissue transglutaminase. *Mol Cell Biol* 21: 148–155

63. Fujio N, Hatayama T, Kinoshita H, Yukioka M (1987) Induction of four heat-shock proteins and their mRNAs in rat after whole-body hyperthermia. *J Biochem* 101: 181–187

64. Nowak TS, Bond U, Schlesinger MJ (1990) Heat shock protects RNA levels in brain and other tissues after hyperthermia and transient ischemia. *J Neurochem* 54: 451–458

65. Abdulrahman BA, Khweek AA, Akhter A, Caution K, Tazi M, Hassan H, Zhang Y, Rowland PD, Malhotra S, Aeffner F *et al* (2013) Depletion of the ubiquitin-binding adaptor molecule SQSTM1/p62 from macrophages harboring cftr DF508 mutation improves the delivery of *Burkholderia cenocepacia* to the autophagic machinery. *J Biol Chem* 288: 2049–2058

66. Ferrari E, Monzani R, Villella VR, Esposito S, Saluzzo F, Rossin F, D'Eletto M, Tosco A, De Gregorio F, Izzo V *et al* (2017) Cysteamine re-establishes the clearance of *Pseudomonas aeruginosa* by macrophages bearing the cystic fibrosis-relevant F508del-CFTR mutation. *Cell Death Dis* 8: e2544

67. Cappellari M, Bielli P, Paronetto MP, Ciccosanti F, Fimia GM, Saarikettu J, Silvennoinen O, Sette C (2014) The transcriptional co-activator SND1 is a novel regulator of alternative splicing in prostate cancer cells. *Oncogene* 33: 3794–3802

68. Cozza G, Girardi C, Ranchio A, Lolli G, Sarno S, Orzeszko A, Kazimierczuk Z, Battistutta R, Ruzzene M, Pinna LA (2014) Cell-permeable dual inhibitors of protein kinases CK2 and PIM-1: structural features and pharmacological potential. *Cell Mol Life Sci* 71: 3173–3185

69. Morris GM, Huey R, Lindstrom W, Sanner MF, Belew RK, Goodsell DS, Olson AJ (2009) Autodock4 and AutoDockTools4: automated docking with selective receptor flexibility. *J Comput Chem* 16: 2785–2791